Al Furat Journal of Innovations in Engineering Applications (AJIEA)

Three Dimensional Cellular Nonlinear Networks (3D-CNNs) Based Image Processing with Complex Patterns and Nonlinear Dynamics with oscillations

Ahmed M. Ali Ali [1*] , Fadhil R. Tahir [2] , Ahmed Fahim Al-Baghdadi [3]

[1] Babylon Technical Institute, Al-Furat Al-Awsat Technical University, Babylon 51001, Iraq
[2] Electrical Engineering Department, University of Basrah, Basrah 61001 , Iraq
[3] Najaf Technical Institute, Al-Furat Al-Awsat Technical University, Babylon 51001, Iraq
[*]Ahmed.ali@atu.edu.iq

Abstract. *Cellular Neural Networks (CNNs) represent one of the most effective computational frameworks for modeling complex spatiotemporal pattern formation in image processing systems. The dynamic behavior of CNN processing units is formally governed by systems of nonlinear differential equations, which articulate the state evolution of individual cells within the network topology A specialized variant, Reaction-Diffusion CNNs (RD-CNNs), extends this paradigm by incorporating reaction-diffusion dynamics inspired by biological systems. This architecture demonstrates remarkable emergent properties, including the spontaneous generation of spiral wave patterns and autowave propagation through locally coupled processing units. Such phenomena enable RD-CNNs to simulate self-organizing patterns observed in natural systems, such as chemical oscillators and neural tissue*

Keywords: *Nonlinear dynamics; CNNs based chaos; RD-CNNs; PWL function.*

1. INTRODUCTION

Numerous artificial, physical, chemical, and biological systems can be effectively built utilizing Cellular Nonlinear Networks (CNNs). Moreover, CNNs represent a strict blocks for complex systems such as image processing tasks [1]. The concept of templates, which symbolizes local activity, is essential for comprehending the functionality of CNNs, hence facilitating the design and modeling of complicated systems. It has extensive applications in image processing, robotics, and biological recognition [2, 3]. It also possesses an enhanced cerebral objective [4, 5]. Additionally, it can serve as a model for executing patterns, spiral, auto, scroll waves, and spatiotemporal chaos. Given that these recent uses are more expansive and not exclusively linked to neural networks, A CNN is a spatial arrangement of locally interconnected cells. Each cell functions as a dynamic model characterized by an input, an output, and a state that evolves according to defined dynamical principles. CNN represents an innovative category of information-processing systems. It is an extensive nonlinear circuit that processes signals in real-time [2]. The CNN comprises a vast array of systematically organized circuit clones, referred to as cells, which interact directly with neighboring cells and indirectly with the entire CNN array through the propagation of continuous-time dynamics inside the cellular nonlinear network. The conventional CNN functions as a parallel analog processor, which manages and produces analog signals for the reproduction and emulation of intricate systems [2]. The cloning templates are crucial to the principle of local activity. Furthermore, RD-CNN serves as a crucial foundation for the intricate dynamics of physical, biological, and chemical systems, particularly for emergent and complicated behavioral patterns[4]. Perez-Munuzuri et al. delineated a two-dimensional CNN array of connected states for spatial recognition [7]. Tang et al. suggested a biological imaging approach utilizing CNNs [8]. Roska and Chua in [9] have affirmed that CNN is a potent paradigm in both artificial and biological applications. Alaa Zaghloul et al. introduced a key generator utilizing one-way coupled map lattice (OCML) for resilient multimedia encryption, including images and audio [10]. Karthikeyan Rajagopal et al. investigated the Hindmarsh–Rose neuron model, focusing on the development of spiral waves within the network, influenced by specific parameters and their coupling strength [11]. Ch. K., Volos et al. in [12] proposed an encryption system founded on two distinct synchronization or coupling events. Price et al. introduced reaction-diffusion equations to model biological phenomena [13]. Jankowski and Wanczuk proposed CNN templates for image processing to enhance distorted images [14]. Setti and Thiran both presented a CNN model to establish spatial and spatiotemporal patterns [15]. In [16], Guodong et al. introduced a convolutional neural network for edge identification, referred to as EDCNN, to delineate the edges of radar cloud pictures. Numerous instances fall into a novel category of dynamical systems based on convolutional neural networks and template training through optimization methods [17-21].

This research presents system models utilizing cellular nonlinear networks (CNNs) to address image processing challenges such as noise reduction, corner recognition, and edge extraction. The reaction-diffusion cellular nonlinear networks (RD-CNNs) are fundamental to the emergence of pattern formations, autonomous waves, and spirals.

2. CNNS THEORY AND METHODS

The CNNs exhibit the most advantageous characteristics [2] as follows:

1. It is a continuous-time characteristic that enables real-time signal processing, which is inadequate in the digital domain.
2. The local linking characteristic renders it appropriate for VLSI implementation.

2.1. Definition 1: Basic CNN Structure

A CNN composed of M×N dimensions that describe of CNN structuew where i = 1, 2, ..., M, j = 1, 2,..., N, see Fig. (1).There are applications where M≠N.

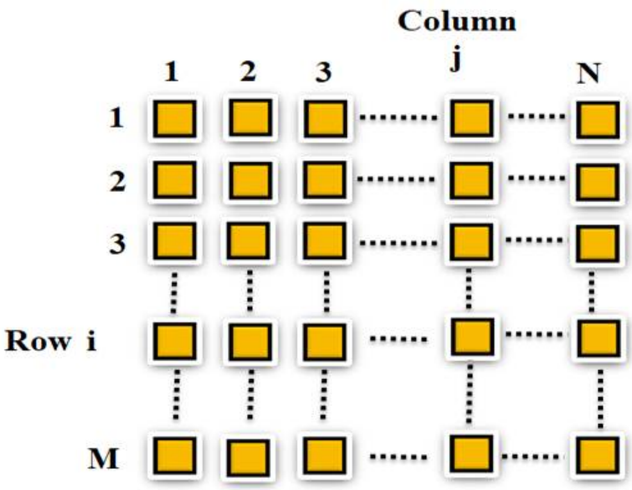

Fig.1 Schematic representation of $M \times N$ CNN of regular 2D-array cells with its local linkage property in Cartesian coordinates.

For example, 1 × N CNN rectangular array for special purposes and 5×512 CNN would be more suitable for imaging or copying [2].

2.2. Definition 1: Basic CNN Structure

The separated CNN cell is used virtually in practical implementation in the CNN chip. The state equation of an isolated cell can be described as following [2, 6]:

$$\frac{d\boldsymbol{X}_{ij}}{dt} = -\boldsymbol{X}_{ij} + a_{ij}\,\boldsymbol{Y}_{ij} + b_{ij}\,\boldsymbol{u}_{ij} + \boldsymbol{Z}_{ij} \quad (1)$$

Where: X_(ij)∈R is called state, Yij ∈R is called output, andY_ij=f(X_ij), u_ij ∈R is called input, z_ij ∈ R is called the threshold of cell C (i,j), a_ij is the center matrix of the feed backward operators or synapses. And b_ij is the center matrix of the feedforward operators or synapses, respectively. The output equation of the standard isolated cell is given by:

$$f(X_{ij}) = \frac{1}{2}\left(|Xij + 1| - |X_{ij} - 1|\right) = \begin{cases} 1 & X_{ij} \geq 1 \\ X_{ij} & |X_{ij}| < 1 \\ -1 & X_{ij} \leq -1 \end{cases} \quad (2)$$

Fig. (2) (a) shows the output equation of CNN, and Fig. (2) (b) shows isolated cell input, output, threshold, and state.

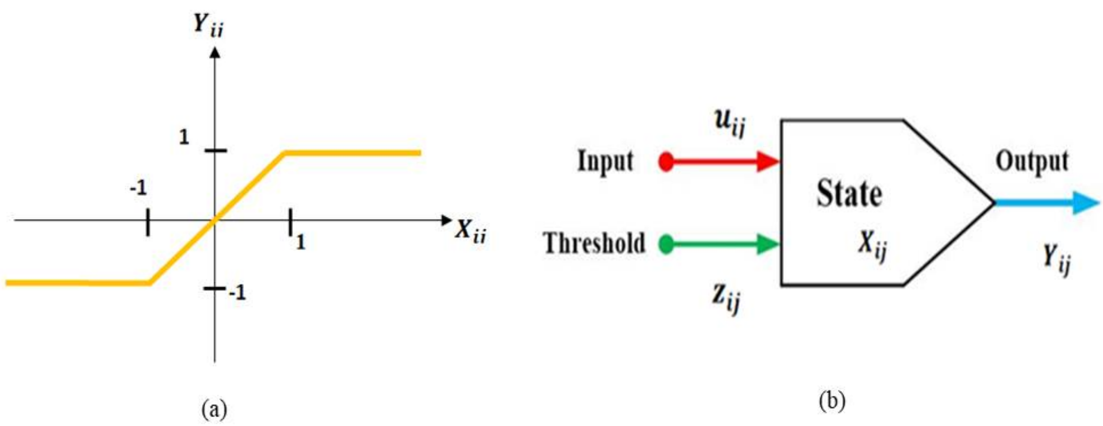

Fig. (2) (a) The output of the isolated cell of PWL function and (b) Isolated cell with input, threshold, and state.

Al Furat Journal of Innovations in Engineering Applications (AJIEA)

2.3. Definition 3: Spherical Effect

Any CNN cell C_ij is, by a qualifier, combined locally to its surrounding cells that found in a spherical effect S_ij (r) of the radius (r), [2, 6]as:

$$S_{ij} = \{C_{ij}: \max(|k-i|, |l-j|) \leq r, 1 \leq k \leq M, 1 \leq N\} \quad (3)$$

Fig. (3)(a) illustrates an array with a radius r= 1. It is commonly called a neighborhood of radius 1, or a 3×3 spherical effect. In such matter, the center cell is companied just “eight” closest neighbor cells C_kl . Where (k,l) = (i + 1,j + 1),(i + 1,j),(i+1,j - 1),(i,j + 1),(i,j - 1),(i –1 ,j + 1),(i - 1,j) and (i - 1,j - 1). A 5 × 5 sphere (corresponding to r = 2) of effect expands the combination up to 24 cells as shown in Fig. (3)(b). Therefore, generally it will refer to S_r (i ,j) as a (2r+1)×(2r+1) neighborhood.

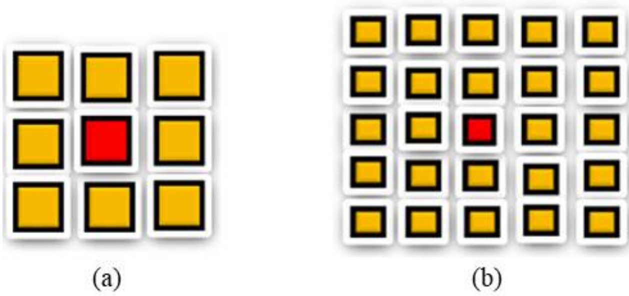

Fig. (3) (a) An array with a radius r=1 (3×3) neighborhood and (b) An array with a radius r=2 (5×5) neighborhood.

2.4. Definition 4: Local Couplings Effects

Generally, in many cases, the input u_kl and the output y_kl of the neighbor cells belonging to the center cell Cij as shown in Fig. (4) (a) and (b). Consequently, it's so suitable to represent every cell in Fig. (4) as a neuron in which the state dynamics are coupled to the cell C_ij . This representation is regarded as a synopsis model of actual neuron cells.

The input u_ij of every neighbor cell C_kl “senses” by a synapse and gives a contribution weight b_(kl) u_kl in the center cell C_ij; therefore, the fundamental contributions that incoming from all the other "eight" closest cells are as:

$$B(u_{ij}) = \sum_{u_{kl} \in S_{ij}, kl \neq ij} b_{kl} u_{kl} \quad (4)$$

As a result, it indicates to “eight” synapses in Fig. (4) (a) as "control" or "feedforward" templates. Similarly, the output y_kl of every closest cell C_kl “senses” by new synapse which is given by:

$$A(y_{ij}) = \sum_{u_{kl} \in S_{ij}, kl \neq ij} a_{kl} y_{kl} \quad (5)$$

The C_ij conducts both weights, which are b_kl u_kl and a_kl y_kl, respectively, from the eight neighbor cells C_kl as in Fig. (4) (a) and (b). Now, by coupling Eq.s (4) and (5) with the right-hand side of Eq. (3), obtaining the standard CNN Eq. (6) given later in this section.

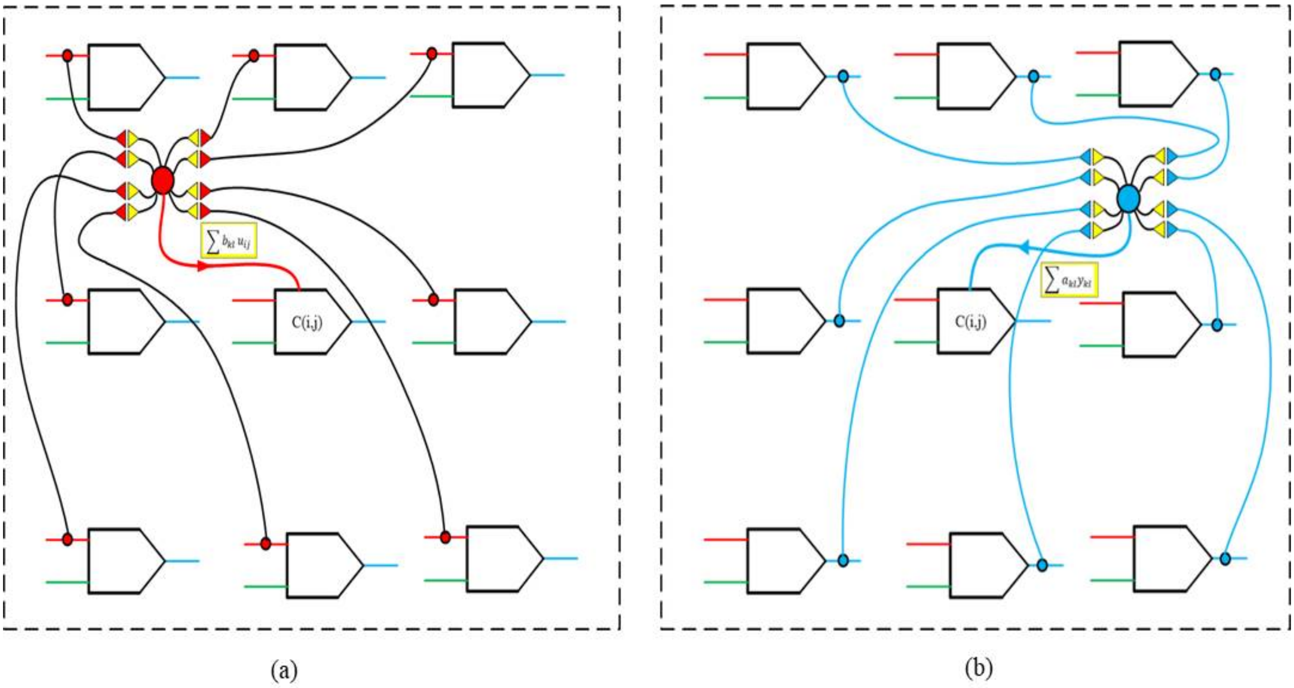

Fig. (4) (a) The weights effect of feedforward synapses and (b) The weights effect of feedback synapses, that whole contributions are incoming from all the other “eight” closest cells

$$\dot{\boldsymbol{X}}_{ij} = -\boldsymbol{X}_{ij} + \sum_{c(k,l) \in S_{ij}(i,j), kl \neq ij} A(i,j;k,l) y_{kl} + \sum_{c(k,l) \in S_{ij}(i,j), kl \neq ij} B(i,j;k,l) u_{kl} + Z_{ij} \quad (6)$$

where i = 1,2,...,M, j = 1,2,...,N.

2.5. Definition5: Spaced-Invariant CNN

If the templates are identical for each cell, they are termed space-invariant; otherwise, they are classified as space-variant. Most CNN applications employed space-invariant CNNs with a 3×3 neighborhood (spherical effect r=1). Considering the standard cell c(i,j)∈ 〖S 〗_r (i,j) as delineated in [1]:

1. Analysis of the feedback synapses operator $A(\,i,j;\;k,l)$, in view of the space-invariance:

$$\sum_{C(k,l)\in S_r(i,j)} A(i,j;k,l)y_{kl} = \sum_{|k-i|\le 1}\sum_{|j-l|\le 1} A(i,j;k,l)y_{kl}$$
$$= a_{-1,-1}\,y_{i-1,j-1} + a_{-1,0}y_{i-1,j} + a_{-1,1}y_{i-1,j+1} + a_{0,-1}y_{i,j-1} + a_{0,0}\,y_{i,j} + a_{0,1}\,y_{i,j+1}$$
$$+ a_{1,-1}y_{i+1,j-1} + a_{1,0}y_{i+1,j} + a_{1,1}y_{i+1,j+1} = \sum_{k=-1}^{1}\sum_{l=-1}^{1} a_{k,l}y_{i+k,j+1} \quad (7)$$

1. The input synaptic operator $B(i,j;k,l)$ similar to the A template. One can write:

$$\sum_{C(k,l)\in S_r(i,j)} B(i,j;k,l)y_{kl} = \sum_{|k-i|\le 1}\sum_{|j-l|\le 1} B(i,j;k,l)u_{kl}$$
$$= b_{-1,-1}\,u_{i-1,j-1} + b_{-1,0}u_{i-1,j} + b_{-1,1}u_{i-1,j+1}b_{0,-1}u_{i,j-1} + b_{0,0}\,u_{i,j} +$$
$$b_{0,1}\,u_{i,j+1} + b_{1,-1}u_{i+1,j-1} + b_{1,0}u_{i+1,j} + b_{1,1}u_{i+1,j+1}$$
$$= \sum_{k=-1}^{1}\sum_{l=-1}^{1} b_{k,l}u_{i+k,j+1} \quad (8)$$

Now, by using the same notations, the space-invariance CNN can be described by:

$$\dot{x}_{ij} = -x_{ij} + \boldsymbol{A} \circledast \boldsymbol{Y_{ij}} + \boldsymbol{B} \circledast \boldsymbol{U_{ij}} + Z \quad (9)$$

So, one can decompose (9) to the following:

$$\dot{x}_{ij} = -x_{ij} + a_{00}\,f(x_{ij}) + \overline{\boldsymbol{A}} \circledast \boldsymbol{Y_{ij}} + \boldsymbol{B} \circledast \boldsymbol{U_{ij}} + Z$$
$$h_{ij}(x_{ij};w_{ij}) = g(x_{ij}) + w_{ij}(x_{ij},t) \quad (10)$$

It is called the rate function, and g(x_ij) is called the driving point (DP), and w_ij (x_ij,t) called Offset level, respectively. Fig. (5) shows such dynamic behavior of Eq.(10).

Al Furat Journal of Innovations in Engineering Applications (AJIEA)

3. RD-CNNS

Spatiotemporal patterns are ubiquitous in physics, biology, and chemistry, frequently arising spontaneously in diverse systems. These features are fostered extensive mathematical modeling, resulting in an enhanced comprehension of many mechanisms. Partial differential equations of diffusion type facilitate pattern creation in several live cells. Certain autonomous CNNs provide an exceptional approximation of nonlinear PDEs, yielding real-time solutions for certain systems [22]. The CNN model's most remarkable feature is its utilization of the cooperative behavior inherent in dynamic nonlinear circuits to accomplish complicated and comprehensive tasks. The creation of 3D-CNN dynamics demonstrates the emergence of compatible surprising shapes, and RD-CNN is appropriate for reintroducing complex phenomena in bioscience, neuro-dynamics, and chemistry. CNN serves as an effective medium for elucidating shapes and patterns related to the emergence of dynamics in systems, as well as for bridging the gap between circuitry and art [23]. The renowned partial differential equation of reaction-diffusion.

$$\frac{\partial \boldsymbol{u}}{\partial t} = F(\boldsymbol{u}) + D\nabla^2 \boldsymbol{u} \tag{11}$$

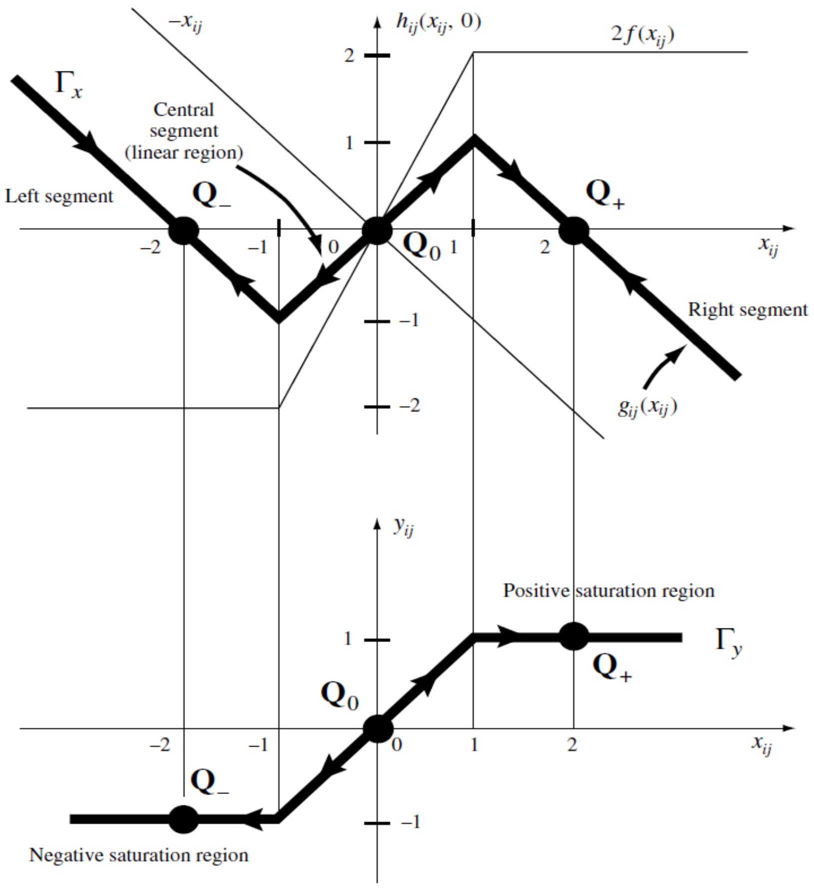

Fig. (5) The dynamics route of both the state x_ij and output Y_ij with a zero offset level (w_ij=0).

Al Furat Journal of Innovations in Engineering Applications (AJIEA)

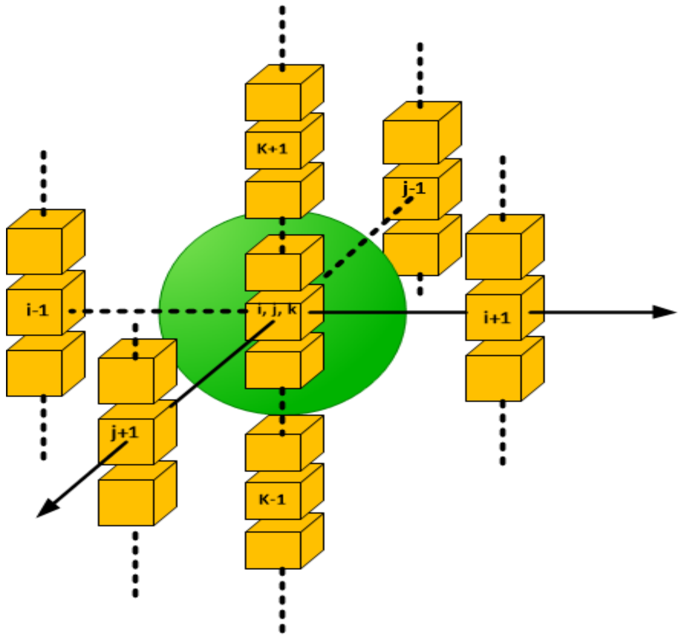

Fig. (6) Schematic depiction of a 3D-CNN array in Cartesian coordinates i, j, k, where each cube signifies an individual cell that interacts physically with others..

Let u∈RNu∈RN and F∈RNF∈RN, with DD denoting a diagonal matrix that models linked diffusion, and ∇2u∇2urepresenting the Laplacian operator in R2R2. Various approaches exist to estimate the discrete form of the Laplacian operator using convolutional neural network (CNN) synaptic laws, typically involving a carefully designed A-template. The 3D-CNN framework necessitates a comprehensive examination of both the architectural configuration and its emergent dynamical behavior. The complex internal dynamics of the system can be interpreted through the integration of 3D-CNN-based shape analysis. Notably, a divergence in the capacity of CNNs to model shape evolution has been observed, where the evolving shape reflects a fractional state within the emergent behavior of nonlinear dynamical systems. Figure 6 provides a graphical illustration of the 3D-CNN structure, where each computational cell is represented as a small cube and the interconnections between them are visually depicted, as discussed in [23].

$$c_{i,j,k}\left(\boldsymbol{x}_{ijk}\right) = D\nabla^2_{ijk}\boldsymbol{x} \tag{12}$$

The discrete Laplacian operator in a three-dimensional spatial configuration is defined by the relation [23].

$$\nabla^2_{ijk}\boldsymbol{x} = \boldsymbol{x}_{i-1,i,k} + \boldsymbol{x}_{i+1,j,k} + \boldsymbol{x}_{i,j-1,k} + \boldsymbol{x}_{i,j+1,k} + \boldsymbol{x}_{i,j,k-1} + \boldsymbol{x}_{i,j,k+1} - 6\boldsymbol{x}_{i,j,k} \tag{13}$$

Based on the aforementioned assumptions, the system of equations (11) can be reformulated [23]:

$$\dot{\boldsymbol{x}}_{\boldsymbol{ijk}} = \boldsymbol{f}\left(\boldsymbol{x}_{\boldsymbol{ijk}}\right) + \boldsymbol{D}\left(\boldsymbol{x}_{\boldsymbol{i-1,j,k}} + \boldsymbol{x}_{\boldsymbol{i+1,j,k}} + \boldsymbol{x}_{\boldsymbol{i,j-1,k}} + \boldsymbol{x}_{\boldsymbol{i,j,k-1}} + \boldsymbol{x}_{\boldsymbol{i,j,k+1}} - \ \boldsymbol{6x}_{\boldsymbol{ijk}}\right) \tag{14}$$

4. CNNS BASED IMAGE PROCESSING APPLICATIONS

The CNNs would represent a general model for a class of circuits for which it reproduces the dynamics. In this thesis, many CNN cell models have been proposed. One of CNN applications is that image processing. Complex pattern formation is one of the interesting phenomena exhibited by CNNs [24].

4.1. Edge Extraction

The aim here is to extract the edge of the input images shown in Fig. (7) (a) and (b), respectively. Where each pixel has at least one white neighbor. By proposing specific cloning templates. The initial conditions are chosen arbitrarily with fixed boundary conditions. So the output image is as shown in Fig. (7) (c) and (d), respectively.

$$A = \begin{bmatrix} 0 & 0 & 0 \\ 0 & 2 & 0 \\ 0 & 0 & 0 \end{bmatrix};\ B = \begin{bmatrix} -1 & -1 & -1 \\ -1 & 8 & -1 \\ -1 & -1 & -1 \end{bmatrix};\ I = -1 \tag{15}$$

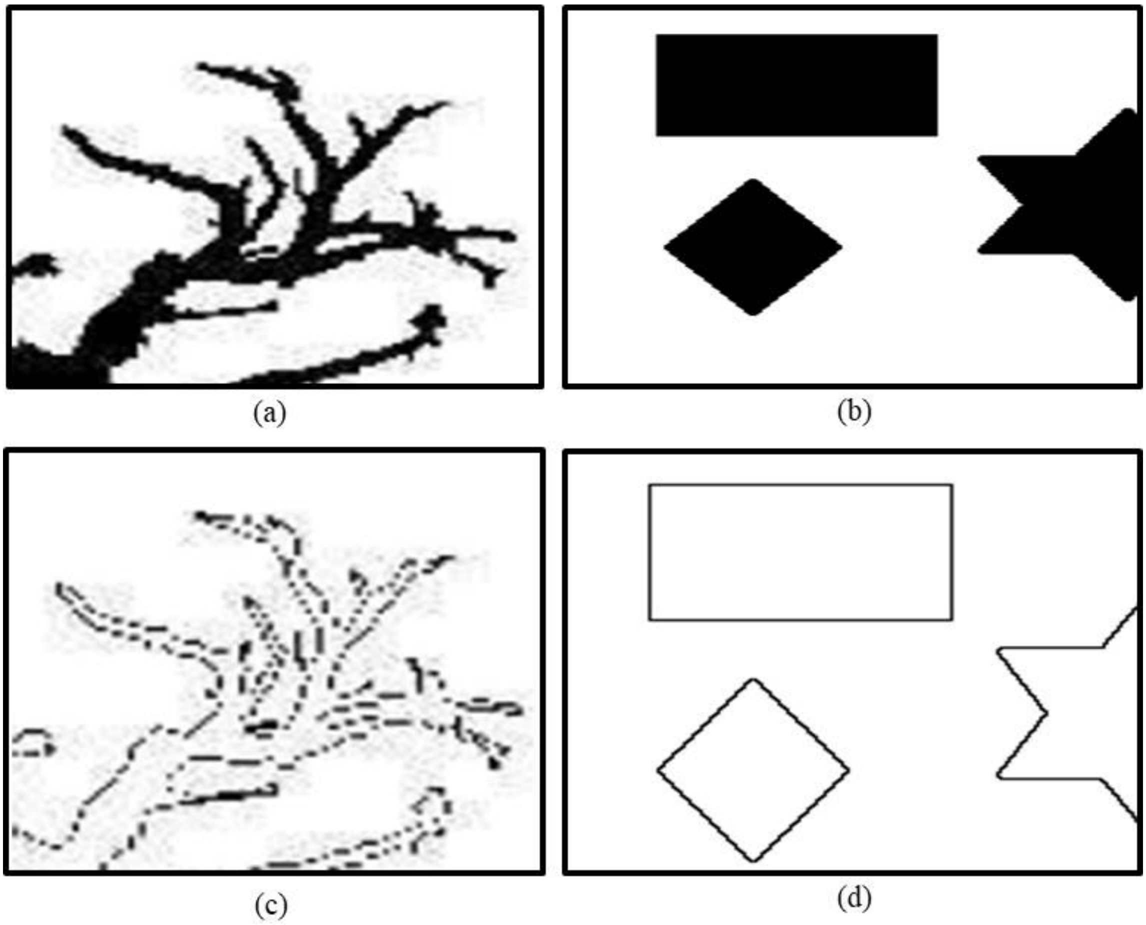

Fig. (7) Edge extraction simulation results (a) and (b) Binary input images. (d) and (c) output images of CNN.

4.2. Corner Detection

The task here is to find the objects' corners by considering black pixels having at least five white neighbors and the input image as shown in Fig. (8)(a). By setting another cloning templates. The initial conditions are chosen arbitrarily with zero-flex boundary conditions. So the output image is as shown in Fig. (8)(b).

$$A = \begin{bmatrix} 0 & 0 & 0 \\ 0 & 1 & 0 \\ 0 & 0 & 0 \end{bmatrix}; B = \begin{bmatrix} -1 & -1 & -1 \\ -1 & 4 & -1 \\ -1 & -1 & -1 \end{bmatrix}; I = -5 \qquad (16)$$

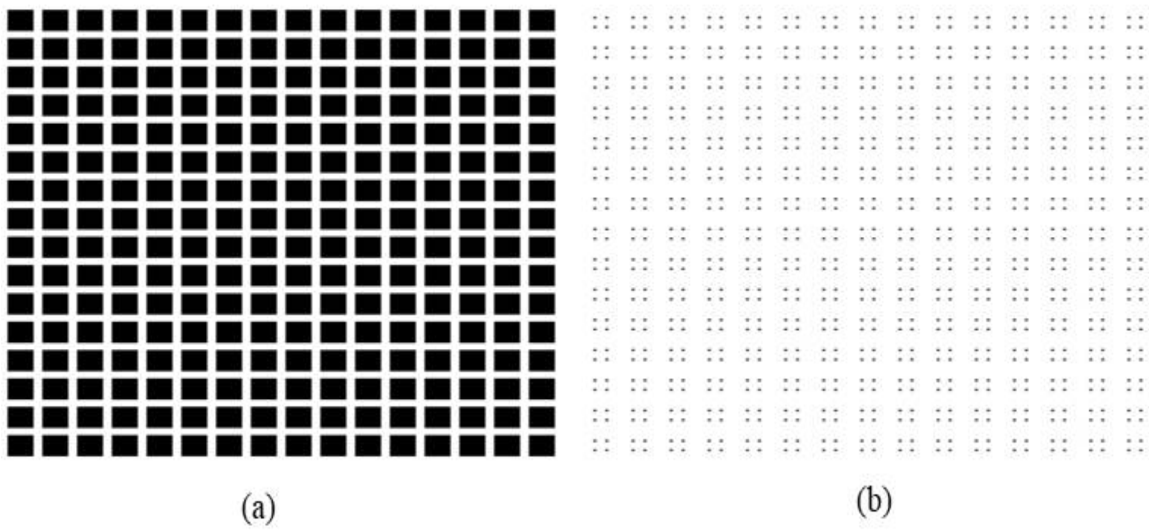

Fig. (8) Corner detection simulation results (a) Input image and (b) Output image of CNN.

4.3. Fogy Removal

To eliminate Gaussian noise from the image shown in Fig. (9)(a) with a set of templates is proposed. The initial conditions are chosen arbitrarily with zero-flex boundary conditions. So the output image is as shown in Fig. (9)(b). The cloning templates are:

$$\text{A}= \begin{bmatrix} 0 & 1 & 0 \\ 1 & 2 & 1 \\ 0 & 1 & 0 \end{bmatrix}; B = \begin{bmatrix} 0 & 0 & 0 \\ 0 & 0 & 0 \\ 0 & 0 & 0 \end{bmatrix}; \; I = 0 \qquad (17)$$

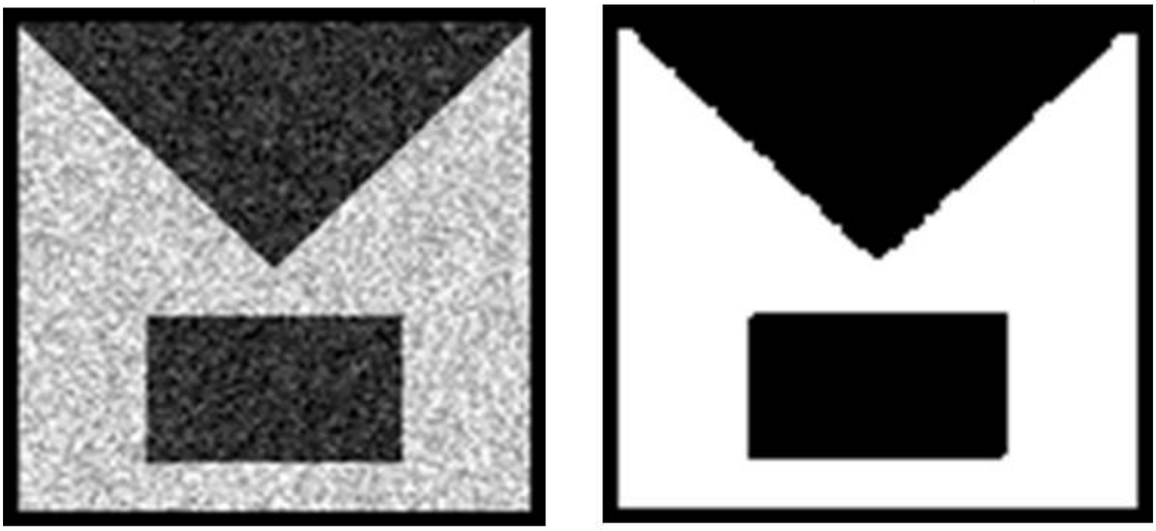

Fig. (9) Gaussian noise removal simulation results (a) Input image and (b) Output image of CNN.

5. REACTION-DIFFUSION CNNS BASED APPLICATIONS

In many cases, every cell's behavior is chaotic and described by low diffusion coefficients, and zero-flux boundary conditions had selected. Rich, unpredictable, and attractive dynamics are associated with the design of the cells of different systems. A chaotic attractor introduces the dynamic system's chaotic behavior is converted to beauty 3D forms such that one is shown in [22]. In practice, many chaotic dynamics systems have been investigated to mimic such networks' global behavior in 3D space like Lorenz, Rossler, and Chua's models or as FitzHugh-Nagumo neuron model in [23].

5.1. Generation of Turning patterns by RD-CNN

The generation of complex patterns in RD-CNN can be obtained by suitably choosing the parameters of the proposed model. By considering specific RD-CNN model. The model is reformulated in the standard CNN. The initial state shown in Fig. (10)(a) and the output shown in Fig. (10)(b).

$$\dot{x}_1 = -x_1 + (1+\mu+\varepsilon)y_1 - sy_2 + i_1 + D_1(y_{1_{i+1,j}} + y_{1_{i-1,j}} + y_{1_{i,j+1}} + y_{1_{i,j-1}} - 4y_{1_{ij}})$$
$$\dot{x}_2 = -x_2 + sy_1 + (1+\mu-\varepsilon)y_2 + i_2 + D_2(y_{2_{i+1,j}} + y_{2_{i-1,j}} + y_{2_{i,j+1}} + y_{2_{i,j-1}} - 4y_{2_{ij}}) \quad (18)$$

with 1≤i≤M and 1≤j≤N.

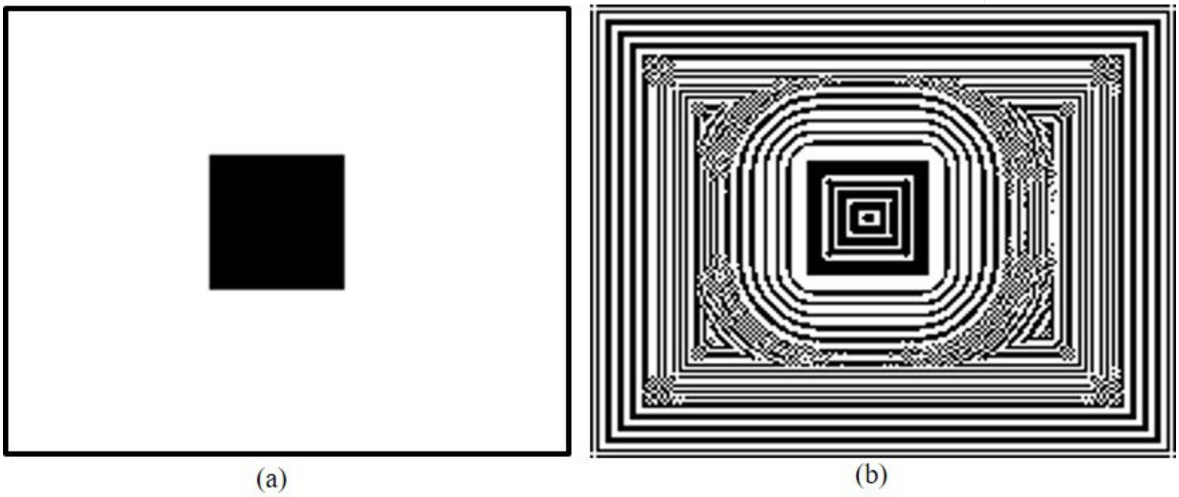

Fig. (10) Generation of turning patterns simulation results (a) Initial state and (b) Output Turing patterns.

5.2. Generation of spiral waves By RD-CNN

To generate a spiral wave, one considers the RD-CNN model (18) with different proposed parameters. Considering the initial states as shown in Fig. (11) (a) and (b), respectively, as the seed of a single wave. The result is a Spatio-temporal phenomenon of propagation in the spiral wave shown in Fig. (11) (c) and (d), respectively.

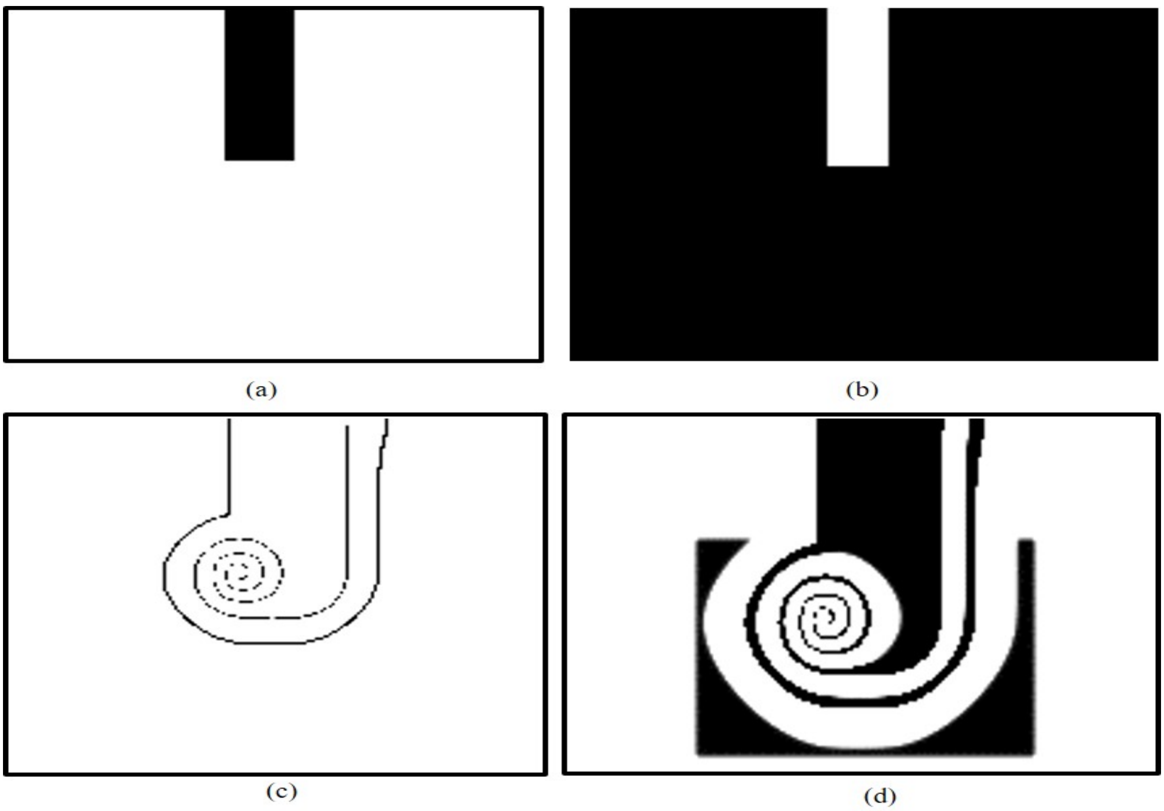

Fig. (11) Spiral wave propagation simulation results (a) and (b) Initial states. (c) Output spiral wave at T=300 Sec. and (d) Output spiral wave at T=1000 Sec.

6. CONCLUSIONS

The shapes in 3D-CNNs are the fingerprint of the emergent phenomena. The approach presented in this paper gives the possibility to obtain many different dynamical models for the observation of nonlinear behavior in complex dynamics. The system has been designed and implemented by using different arrays cells of CNN using MATLAB environment. The simulation results had demonstrated a good approximation of the behavior of such complex systems based on CNNs with high percentage of enhacement. The RD-CNNs can be regarded as vector coupled oscillators as spiral wave propagation. All the above spiral waves, and patterns can be used with secured communication systems and military applications.

REFERENCES

[1] L. O. Chua and L. Yang, “Cellular neural networks: Theory,” IEEE Transactions on Circuits and Systems, vol. 35, no. 10, pp. 1257–1272, 1988.

[2] L. O. Chua and L. Yang, “Cellular neural networks: Applications,” IEEE Transactions on Circuits and Systems, vol. 35, no. 10, pp. 1273–1290, 1988.

[3] A. Kananen et al., “CNN applications from the hardware point of view: Video sequence segmentation,” International Journal of Circuit Theory and Applications, vol. 30, no. 2–3, pp. 117–137, 2002.

[4] L. O. Chua, “CNN: A vision of complexity,” International Journal of Bifurcation and Chaos, vol. 7, no. 10, pp. 2219–2425, 1997.

[5] L. Orzó et al., CNN model of the feature-linked synchronized activities in the visual thalamo-cortical system, Research Report of the Neuromorphic Information Technology Graduate Center, NIT-2-1966, 1996.

[6] L. O. Chua and T. Roska, Cellular neural networks and visual computing: Foundations and applications. Cambridge, U.K.: Cambridge Univ. Press, 2002.

[7] V. Perez-Munuzuri et al., “Autowaves for image processing on a two-dimensional CNN array of excitable nonlinear circuits: Flat and wrinkled labyrinths,” IEEE Transactions on Circuits and Systems I: Fundamental Theory and Applications, vol. 40, no. 3, pp. 174–181, 1993.

[8] S.-S. Tang, K.-L. Fei, and W. Wang, “Biomedical image edge detection based on CNN,” in Proc. 2017 Int. Conf. Wireless Commun., Networking and Applications, 2017.

[9] T. Roska and L. O. Chua, “Cellular neural networks with non-linear and delay-type template elements and non-uniform grids,” International Journal of Circuit Theory and Applications, vol. 20, no. 5, pp. 469–481, 1992.

[10] A. Zaghloul et al., “A block encryption scheme for secure still visual data based on one-way coupled map lattice,” Journal of Information Security and Applications, vol. 8, no. 4, pp. 89–100, 2014.

[11] K. Rajagopal et al., “Wave propagation and spiral wave formation in a Hindmarsh–Rose neuron model with fractional-order threshold memristor synapse,” Chaos, Solitons & Fractals, vol. 34, no. 17, p. 2050157, 2020.

[12] C. K. Volos, I. M. Kyprianidis, and I. N. Stouboulos, “Image encryption process based on chaotic synchronization phenomena,” Signal Processing, vol. 93, no. 5, pp. 1328–1340, 2013.

[13] C. Price, P. Wambacq, and A. Oosterlinck, “The reaction-diffusion cellular neural network,” in Proc. CNNA’92 2nd Int. Workshop Cellular Neural Networks and Their Applications, 1992, IEEE.

[14] S. Jankowski and R. Wanczuk, “Nonlinear CNN cloning templates for image thickening,” in Proc. CNNA’92 2nd Int. Workshop Cellular Neural Networks and Their Applications, 1992, IEEE.

[15] G. Setti and P. Thiran, “Biological pattern formation with cellular neural networks,” in Proc. CNNA’96 4th IEEE Int. Workshop Cellular Neural Networks and Their Applications, 1996, IEEE.

[16] G. Guodong et al., “A method analysis for hail cloudy prediction based on CNN,” Neural Computing and Applications, vol. 19, no. 4, pp. 2015–2026, 2016.

[17] H. M. Özer et al., “Bayesian estimation of discrete-time cellular neural network coefficients,” International Journal of Circuit Theory and Applications, vol. 25, no. 3, pp. 2363–2374, 2017.

[18] B. Luitel and G. K. Venayagamoorthy, “Decentralized asynchronous learning in cellular neural networks,” IEEE Transactions on Neural Networks and Learning Systems, vol. 23, no. 11, pp. 1755–1766, 2012.

[19] Y. Kato et al., “Four-layer cellular neural networks in consideration of color and luminosity,” in Proc. 2011 20th Eur. Conf. Circuit Theory and Design (ECCTD), 2011, IEEE.

[20] S. Morfu, “Image processing with a cellular nonlinear network,” Physics Letters A, vol. 343, no. 4, pp. 281–292, 2005.

[21] L. Fortuna et al., “Cellular neural networks: A paradigm for nonlinear spatio-temporal processing,” Circuits, Systems and Signal Processing, vol. 1, no. 4, pp. 6–21, 2001.

[22] A. Slavova, “Reaction-diffusion cellular neural network models,” in Proc. 9th WSEAS Int. Conf. Neural Networks (NN’08), Sofia, Bulgaria, 2008.

[23] P. Arena et al., “The CNN paradigm: Shapes and complexity,” International Journal of Bifurcation and Chaos, vol. 15, no. 7, pp. 2063–2090, 2005.

[24] M. Itoh and L. O. Chua, “Equivalent CNN cell models and patterns,” International Journal of Bifurcation and Chaos, vol. 13, no. 5, pp. 1055–1161, 2003.